

## Propagating EUV disturbances in the Solar corona: Two-wavelength observations

D. B. King<sup>1</sup>, V. M. Nakariakov<sup>1</sup>, E. E. Deluca<sup>2</sup>, L. Golub<sup>2</sup>, and K. G. McClements<sup>3</sup>

<sup>1</sup> Physics Department, University of Warwick, Coventry, CV4 7AL, UK

e-mail: kingd@astro.warwick.ac.uk; valery@astro.warwick.ac.uk

<sup>2</sup> Harvard-Smithsonian Astrophysical Observatory, 60 Garden Street, Cambridge, MA02138, USA

e-mail: deluca@head-cfa.harvard.edu

<sup>3</sup> UKAEA Culham Division, Culham Science Centre, Abingdon, Oxfordshire, OX14 3DB, USA

e-mail: k.g.mcclements@ukaea.org.uk

Received 23 January 2003 / Accepted 19 March 2003

**Abstract.** Quasi-periodic EUV disturbances simultaneously observed in 171 Å and 195 Å TRACE bandpasses propagating outwardly in a fan-like magnetic structure of a coronal active region are analysed. Time series of disturbances observed in the different bandpasses have a relatively high correlation coefficient (up to about 0.7). The correlation has a tendency to decrease with distance along the structure: this is consistent with an interpretation of the disturbances in terms of parallel-propagating slow magnetoacoustic waves. The wavelet analysis does not show a significant difference between waves observed in different bandpasses. Periodic patterns of two distinct periods: 2–3 min and 5–8 min are detected in both bandpasses, existing simultaneously and at the same distance along the loop, suggesting the nonlinear generation of the second harmonics.

**Key words.** magnetohydrodynamics (MHD)– waves – Sun: activity – Sun: corona – Sun: oscillations – Sun: UV radiation

### 1. Introduction

Quasi-periodic disturbances of extreme-ultraviolet (EUV) emission, propagating along coronal loops, were discovered by Berghmans & Clette (1999) using the SOHO/EIT instrument. The same phenomenon is believed to have been observed with the TRACE telescope by Nightingale et al. (1999), De Moortel et al. (2000), Berghmans et al. (2001).

Very recently, De Moortel et al. (2002a–c) have studied 38 TRACE examples of this phenomenon and found that the EUV propagating disturbances are often positioned over sunspots. Typically, the disturbances propagate outwards from the sunspot, along the fan-like magnetic structure, at an almost constant speed of about 25–165 km s<sup>-1</sup>. The amplitude of the emission intensity perturbations is usually less than 12% of the background. The characteristic periods are several hundred seconds (180–600 s). Similar periodicities have recently been observed in the coronal green line (Sakurai et al. 2002). According to De Moortel et al. (2002a–c), shorter period disturbances are usually observed over the sunspots, while longer period disturbances normally propagate along loops which are not associated with sunspots. No manifestation of downward

propagation has been found. There is no correlation between the amplitudes, periods and speeds (Nakariakov et al. 2002).

Nakariakov et al. (2000) and Tsiklauri & Nakariakov (2001) developed a model interpreting the EUV propagating disturbances in terms of slow magnetoacoustic waves. Wave propagation in the model is restricted to the magnetic field direction: this is consistent with the fact that the observed disturbances appear to follow diverging magnetic field lines. Slow waves of the observed periodicities (shorter than 20 min) can propagate without reflection in the 1.0 MK corona, as the acoustic cut-off period is about 70 min. According to the model, the waves propagate at about the sound speed in the loop. The observed speed of the waves is reduced by line-of-sight effects.

The first study of propagating EUV disturbances observed *simultaneously* in the 171 Å bandpass using TRACE and the 195 Å bandpass using SOHO/EIT was undertaken by Robbrecht et al. (2001). This investigation showed that the disturbances observed in the different bandpasses by the two telescopes were poorly correlated and that the speeds of the disturbances in 195 Å corresponding to the hotter temperature, were systematically faster than those observed in the cooler 171 Å bandpass (although the difference in speeds was less than the observational uncertainties in each). In this paper we analyse observations from July 2 1998,

---

Send offprint requests to: D. B. King,  
e-mail: kingd@astro.warwick.ac.uk

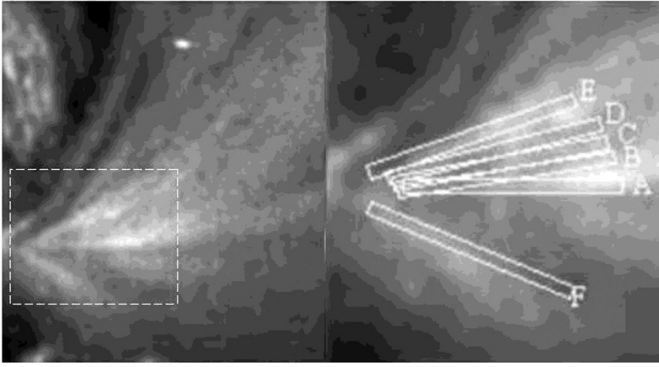


**Fig. 1.** Left panel: active region AR8253 observed by TRACE on July 2 1998 at 06:00 UT in the 195 Å bandpass. Right panel: positioning of the slits on an enlarged image of the region indicated by dashes in the left panel.

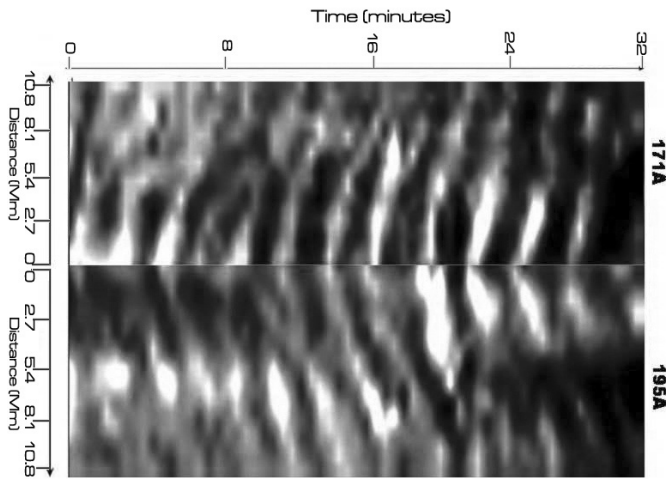


**Fig. 2.** Simultaneous time-distance plots of propagating EUV disturbances observed by TRACE in the 171 Å and 195 Å bandpasses along slit A. The distance along the slit is shown in opposite directions to demonstrate that the disturbances observed in different bandpasses form a “fishbone” structure. This image is taken from the data without interpolation.

when quasi-periodic disturbances were simultaneously observed in the 171 Å and 195 Å bandpasses by the same imaging telescope, TRACE.

## 2. Simultaneous observations of propagating EUV disturbances in 171 Å and 195 Å TRACE bandpasses

On July 2 1998 TRACE observed the on-disk active region AR8253 in the 171 Å and 195 Å bandpasses. A part of the active region with a typical fan-like set of diverging coronal loops is shown in the left panel of Fig. 1. The observation cadence time in both bandpasses was 31 s, and the delay time between observations in 195 Å and 171 Å was 11 s. After 06:01 UT, for about an hour, in both EUV bandpasses outwardly propagating disturbances of the emission intensity were clearly observed. The waves were observed to begin near the origin of the magnetic fan and spread out up to 10 Mm. The intensities measured in both bandpasses, along the same chosen path (Fig. 1,

right panel), were taken at different instants of time and laid side-by-side to form time–distance maps (see DeForest & Gurman 1998 for description of the method). Figure 2 shows a time–distance map constructed for slit A, with distance from the origin shown in opposite directions. A typical “fishbone” structure can be clearly seen, suggesting that the propagating disturbances observed in different bandpasses are highly correlated.

The diagonal stripes of EUV brightness correspond to propagating EUV disturbances. As in the case of all previous observations of this phenomenon, the disturbances are seen to propagate outwardly. The speed of the disturbances was found by fitting the distance variation to a sinusoidal function and locating the maximum. Such maxima are found for each frame and then plotted against the time of each frame. The gradient of this plot gives the velocity component of the disturbances transverse to the line of sight as about 25–40 km s<sup>−1</sup>. The temperatures associated with the 171 Å and 195 Å TRACE bandpasses are 1.0 and 1.6 MK, respectively, which correspond to the sound speeds of 152 km s<sup>−1</sup> and 192 km s<sup>−1</sup>. Assuming the angle between the line of sight (LOS) and the wave vector to be 10–15°, we obtain propagation speeds of the observed propagating disturbances of 150–190 km s<sup>−1</sup>. The disturbances are observed to be quasi-periodic, with the characteristic period of several min.

### 2.1. Correlation analysis

The time–distance maps in Fig. 2 appear to be very similar for the two bandpasses, indicating a high correlation between the propagating disturbances. To quantify this, we performed a correlation analysis of EUV disturbances observed in the two bandpasses propagating along the same slit. For each pixel along a slit, we obtained two time series describing the evolution of the EUV emission intensity and computed the correlation coefficient  $\mathcal{R}$  of these time series (for a precise definition of  $\mathcal{R}$ , see e.g. Kendall & Stuart 1961). The dependence of the correlation coefficient  $\mathcal{R}$  on the pixel position along the slit is shown in Fig. 3. The correlation is quite high for all slits analysed. In five out of six cases studied  $\mathcal{R}$  decreases systematically with distance along the slit.

The high correlation can be caused by low-period components of the spectrum. To exclude this possibility, we calculated also the correlation of the signals, subtracting the low-period component. The filtered signals show the high correlation with each other too.

### 2.2. Wavelet analysis: Evolution of the wave spectrum

Wavelet transforms provide a useful alternative to Fourier transforms for the decomposition of time series exhibiting non-stationary behaviour: it has been applied to the analysis of fluctuations in both laboratory (e.g. Han et al. 2000) and solar (e.g. Ofman et al. 2000; Ireland & De Moortel 2002) plasmas. The TRACE EUV data was analysed in both bandpasses using Morlet wavelet transforms to determine how the wave periods varied with time and along the loop. The intensities of the signal were summed over each 3 neighbouring pixels along the

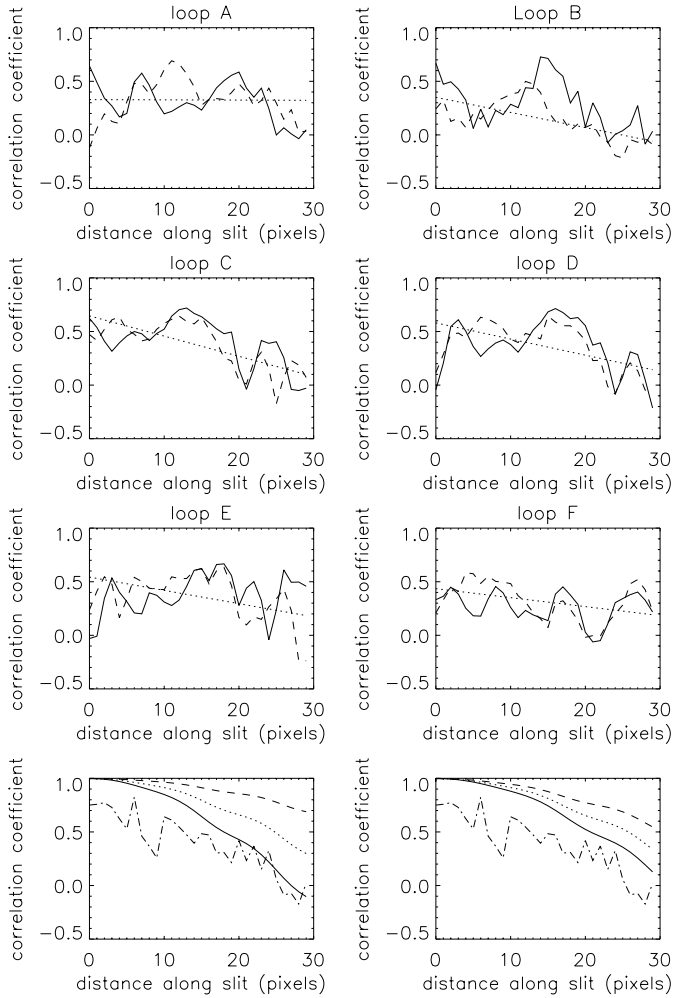


**Fig. 3.** Six upper panels: evolution of correlation coefficients of propagating disturbances observed simultaneously in 171 Å and 195 Å bandpasses with the distance along six different slits (see Fig. 1). The solid lines show the correlation of unfiltered data and the dashed lines – the correlation of the signals after subtraction of slower variation. The dotted lines are the best-fitted straight lines. Two lower panels: evolution of correlation coefficients of simulated signals. The left shows the correlation for the same angle with the line of sight, but for different temperatures  $T_{171} = 1.05, 1.15$  and  $1.2$  MK and  $T_{195} = 1.55, 1.55$  and  $1.45$  MK for the solid, dotted and the dashed line respectively. The right panel shows varying angle  $\theta_{171} = 15^\circ$  and  $\theta_{195} = 15^\circ, 14.5^\circ$  and  $14^\circ$  for the solid, dotted and dashed lines respectively, while keeping the temperature the same. The dot-dash line in each is the correlation of the simulated signals with amplitude noise added.

slit and then the wavelet analysis performed on each of these larger pixels.

Typical results of the wavelet analysis of propagating disturbances observed in both EUV bandpasses are shown in Fig. 4. The lower frequency spectral components were much more intense than the high frequency components, hence they needed to be filtered using a high pass filter method to allow the analysis of the high frequency part of the wave spectrum. Unfortunately, the steady detection of the periodic pattern with satisfactory confidence is not possible because of the high noise level in the signal analysed. However, the wavelet

approach shows the presence of periodic patterns with two distinct period: 2–3 min and 5–8 min in both bandpasses. As both the periodicities are observed simultaneously and at the same positions, one possibility is that the shorter period is the second harmonic of the longer period, suggesting that the propagating disturbances can experience nonlinear steepening. This is consistent with the theoretical model of slow magnetoacoustic waves propagating along coronal loops developed by Nakariakov et al. (2000). Another possibility is that they could be due to direct excitation at these frequencies as 3 and 5 min oscillations are often detected in sunspots.

### 3. Discussion

In contrast with the results of Robbrecht et al. (2001), the propagating disturbances observed in different EUV bandpasses show relatively high correlation. If the two bandpasses observe the same plasma then the high correlation is naturally explained, it is however more difficult to explain a decreasing correlation along diverging field lines for a homogenous plasma, hence small scale temperature mixing is less likely to be responsible for the effect. The systematic decrease in correlation coefficient with distance along the loop may be explained in terms of phase mixing of the waves. If the intensity variations are produced by parallel-propagating slow magnetoacoustic waves, their speed depends only on the temperature corresponding to the bandpass. Consequently, the speeds of the EUV propagating disturbances observed in different bandpasses should be different provided the plasmas observed in different bandpasses have different temperatures. The initially high correlation suggests that the disturbances observed in different bandpasses are generated by the same mechanism.

When the waves are synchronically excited at an origin and then propagate along the *same path* from the origin at different speeds, their correlation decreases with distance from the origin. The actual variation of the correlation is determined by two effects: the difference in phase speeds of the waves observed in the two bandpasses; and the difference (if any) in the LOS angles formed by the structures supporting the waves. These two mechanism can actually work together. To quantify the extent of phase mixing and consequent variation of the correlation coefficient, we simulate the propagating disturbances observed in different bandpasses as harmonic waves generated in phase at the same initial position and propagating at different speeds from the origin,

$$i_\alpha = A_\alpha \sin \left[ \frac{2\pi}{P} \left( t - \frac{s}{C_\alpha \sin \theta_\alpha} \right) \right], \quad (1)$$

where  $i_\alpha$ ,  $A_\alpha$  and  $C_\alpha$  are respectively the intensities, amplitudes and speeds of the waves observed in the two bandpasses (labelled by the index  $\alpha$ ),  $P$  is the wave period, and  $\theta_\alpha$  is the angle between the LOS and the actual direction of the loop. In general, the angles are different for different bandpasses. However,  $\theta_\alpha$  is assumed to be constant for a given passband and a given loop, i.e. we assume that loop curvature can be neglected over the region in which EUV emission is occurring.

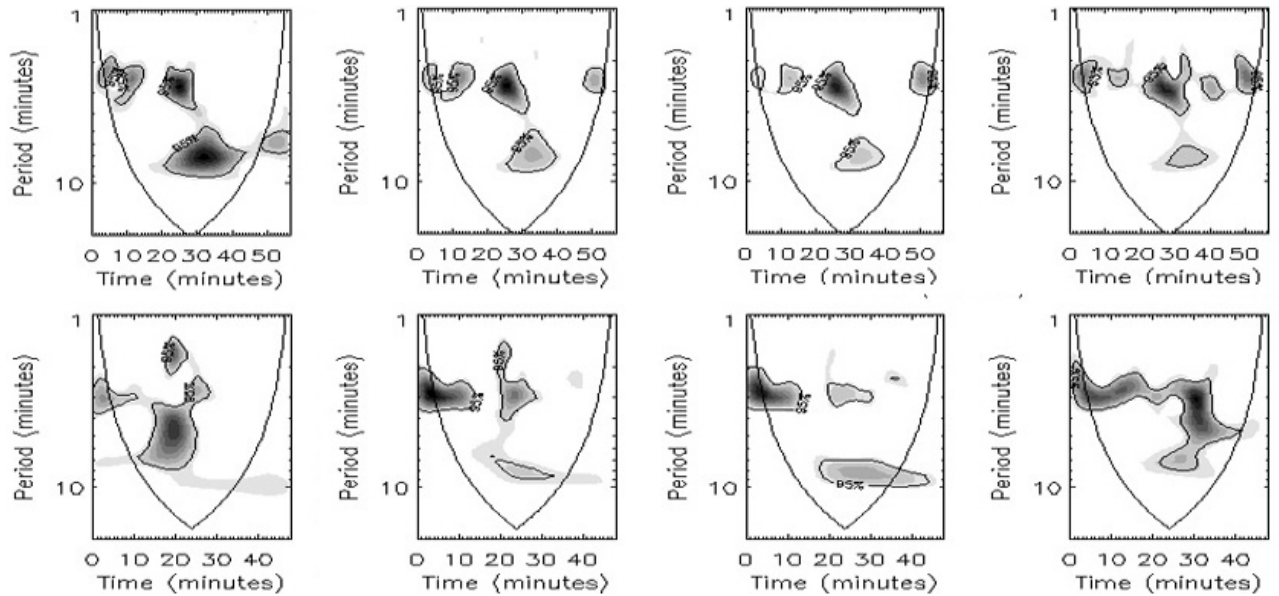


**Fig. 4.** Morlet wavelet transforms of the intensity variation observed at certain fixed points in 171 Å (the upper row) and 195 Å (the lower row) bandpasses. Only periods within the 95% confidence curves are significant.

We also assume that the amplitudes  $A_\alpha$  contain two components: the regular one, corresponding to the actual amplitude of the perturbation, and a random one, simulating the effect of a high frequency noise in the signal, which cannot be filtered out. In the simulations, we assume that the signal to noise ratio is about two. The evolution of the correlation coefficients for different angles  $\theta_\alpha$  and speeds  $C_\alpha$ , as well as with and without the noise, is shown on the two lower panels of Fig. 3. The results of the simulation are consistent with the observations.

We conclude that we observe slow magnetoacoustic waves propagating upwards along diverging magnetic field lines. Wavelet analysis shows the evidence of the presence of the second harmonics. This may be the first direct observation of a nonlinear wave phenomenon in the solar corona. Higher resolution, simultaneous, multi-wavelength observations will allow the exploration of wave propagation to greater heights and at higher frequencies. These wave's role in the coronal energy budget is yet to be determined. The Solar Dynamics Observatory will provide better time resolution, but further improvements in spatial resolution await new missions.

*Acknowledgements.* The Wavelet software was provided by C. Torrence and G. Compo, and is available at URL: <http://paos.colorado.edu/research/wavelets/>.

DBK was supported by a PPARC CASE studentship, and the work was also funded partly by the UK Department of Trade and Industry. The authors are grateful to Leon Ofman for valuable comments.

## References

- Berghmans, D., & Clette, F. 1999, *Sol. Phys.*, 186, 207  
 Berghmans, D., McKenzie, D., & Clette, F. 2001, *A&A*, 369, 291  
 DeForest, C. E., & Gurman, J. B. 1998, *ApJ*, 501, L217  
 De Moortel, I., Ireland, J., Walsh, R. W., & Hood, A. W. 2002a, *Sol. Phys.*, 209, 61  
 De Moortel, I., Hood, A. W., Ireland, J., & Walsh, R. W. 2002b, *Sol. Phys.*, 209, 89  
 De Moortel, I., Ireland, J., Hood, A. W., & Walsh, R. W. 2002, *A&A*, 387, L13  
 De Moortel, I., Ireland, J., & Walsh, R. W. 2000, *A&A*, 355, L23  
 Han, W. E., Thyagaraja, A., Fielding, S. J., & Valovič, M. 2000, *Plasma Phys. Control. Fusion*, 42, 181  
 Ireland, J., & De Moortel, I. 2002, *A&A*, 391, 339  
 Kendall, M. G., Stuart, A. 1961, *The Advanced Theory of Statistics* (London: Griffin)  
 Nakariakov, V. M., King, D. B., & Tsiklauri, D. 2002, *ESA SP-506*, 705  
 Nakariakov, V. M., Verwichte, E., Berghmans, D., & Robbrecht, E. 2000, *A&A*, 362, 1151  
 Nightingale, R. W., Aschwanden, M. J., & Hurlburt, N. E. 1999, *Sol. Phys.*, 190, 249  
 Ofman, L., Romolli, M., Poletto, G., Noci, G., & Kohl, J. L. 2000, *ApJ*, 529, 592  
 Robbrecht, E., Verwichte, E., Berghmans, D., et al. 2001, *A&A*, 370, 591  
 Sakurai, T., Ichimoto, K., Raju, K. P., & Singh, J. 2002, *Sol. Phys.*, 209, 265  
 Tsiklauri, D., & Nakariakov, V. M. 2001, *A&A*, 379, 1106